

Article

# Application of PANI/TiO<sub>2</sub> Composite for Photocatalytic Degradation of Contaminants from Aqueous Solution

Youn-Jun Lee <sup>1</sup>, Hae Su Lee <sup>1</sup>, Chang-Gu Lee <sup>1,\*</sup>, Seong-Jik Park <sup>2</sup>, Jechan Lee <sup>1</sup>,  
Seungho Jung <sup>1,\*</sup> and Gwy-Am Shin <sup>1</sup>

<sup>1</sup> Department of Environmental and Safety Engineering, Ajou University, Suwon 16499, Korea; duswnss@ajou.ac.kr (Y.-J.L.); haesu0318@ajou.ac.kr (H.S.L.); jlee83@ajou.ac.kr (J.L.); gwyam@ajou.ac.kr (G.-A.S.)

<sup>2</sup> Department of Bioresources and Rural System Engineering, Hankyong National University, Anseong 17579, Korea; parkseongjik@hknu.ac.kr

\* Correspondence: changgu@ajou.ac.kr (C.-G.L.); processsafety@ajou.ac.kr (S.J.);  
Tel.: +82-31-219-2405 (C.-G.L.); +82-31-219-2401 (S.J.)

Received: 26 August 2020; Accepted: 24 September 2020; Published: 25 September 2020



**Abstract:** Polyaniline (PANI) is a promising conducting polymer for surface modification of TiO<sub>2</sub> to achieve extended photoresponse to visible light and increased photocatalytic efficiency. In this study, we report the synthesis of a PANI/TiO<sub>2</sub> composite with different weight ratios of PANI, which was subsequently employed for photocatalytic degradation of methylene blue (MB), bisphenol A (BPA), and bacteriophage MS2 under visible-light irradiation. The functional groups, morphology, and light response of the composite were characterized by Fourier-transform infrared spectroscopy, field-emission transmission electron microscopy, and diffuse reflectance UV–visible spectroscopy, respectively. The PANI/TiO<sub>2</sub> composite containing 4% by weight ratio of PANI was most suitable for MB degradation, and this photocatalyst was very stable even after repeated use (four cycles). The degradation of BPA and bacteriophage MS2 by PANI/TiO<sub>2</sub> composite reached 80% in 360 min and 96.2% in 120 min, respectively, under visible-light irradiation. Therefore, the PANI/TiO<sub>2</sub> composite with enhanced visible-light photocatalytic efficiency and stability can be widely used for the degradation of water contaminants.

**Keywords:** polyaniline; titanium dioxide; photocatalyst; visible-light irradiation; water contaminant

## 1. Introduction

Since the first reports on the photoelectrolytic water splitting of titanium dioxide (TiO<sub>2</sub>) by Fujishima and Honda in 1972, photocatalysis has been recognized as an effective technique for the degradation of water contaminants over the past decades [1,2]. Among the semiconductors for photocatalysis, TiO<sub>2</sub>-based nanomaterials are most widely used because of their high efficiency, low cost, mechanical robustness, chemical stability, and non-corrosive property [3,4]. However, the wide-band-gap energy (3.2 eV) that is only photoactive under ultraviolet (UV) light ( $\lambda < 366$  nm) and the relatively high recombination rate of electron-hole pairs restrict the photocatalytic activity of TiO<sub>2</sub> [5].

Visible-light-response photocatalysts provide a popular way to solve environmental problems by directly harvesting energy from sunlight [6]. In this regard, much effort has been made to extend the photo-response region of TiO<sub>2</sub> to visible light and to increase its photocatalytic efficiency under UV and visible-light irradiation by surface modification, such as metal loading, impurity doping, inorganic adsorbates, polymer coating, dye sensitization, and charge-transfer complexation [7].

Among the surface modification methods for oxide-based semiconductors, conducting polymers have attracted much attention owing to their high conductivity and stability, simple synthesis, and excellent environmental compatibility [8]. With an extended  $\pi$ -conjugated electron system, the conducting polymer acts as a stable photosensitizer to sensitize  $\text{TiO}_2$  by the absorption of a wide spectrum of UV and visible-light (190–800 nm) irradiation [5].  $\text{TiO}_2$  modified with conducting polymers, such as polyaniline (PANI), polypyrrole, and polythiophene, has demonstrated excellent photocatalytic activity for the degradation of contaminants under visible-light irradiation [5,9,10].

Especially, PANI has been widely used as a conducting polymer in semiconductor modification because of its high stability, low cost, and easy polymerization [11]. In addition, it has also been regarded as a promising material to overcome the inherent drawbacks of  $\text{TiO}_2$  by facilitating charge (electron-hole) transport due to its well-matched energy level.  $\text{TiO}_2$  is a typical n-type semiconductor, whereas PANI is generally considered a p-type semiconductor [5]. Thus, their strategic combination provides excellent stability and conductivity, as well as enhanced photocatalytic performance. There are several reports on the manufacture, properties, and applications of PANI/ $\text{TiO}_2$  composite for photocatalytic degradation of water contaminants [5,12,13].

Here, we demonstrate the enhanced photocatalytic efficiency of PANI/ $\text{TiO}_2$  composite under visible-light irradiation for degradation of water contaminants (methylene blue (MB), bisphenol A (BPA), and bacteriophage MS2). The PANI/ $\text{TiO}_2$  composites were prepared using different PANI to  $\text{TiO}_2$  weight ratios, and their performance was evaluated by photocatalytic dye degradation experiments. The properties of the prepared samples were analyzed. The applicability and reusability of PANI/ $\text{TiO}_2$  composites were also evaluated.

## 2. Material and Methods

### 2.1. Chemicals

$\text{TiO}_2$  ( $\geq 99.5\%$ ), aniline ( $\text{C}_6\text{H}_5\text{NH}_2$ ,  $\geq 99\%$ ), BPA ( $\text{C}_{15}\text{H}_{16}\text{O}_2$ ,  $\geq 99\%$ ), and ammonium persulfate ( $\text{H}_8\text{N}_2\text{O}_8\text{S}_2$ ,  $\geq 98\%$ ) were purchased from Sigma–Aldrich Co., Ltd. (St. Louis, MO, USA). MB ( $\text{C}_{16}\text{H}_{18}\text{ClN}_3\text{S}$ ,  $\geq 96\%$ ) and hydrochloric acid (HCl, 36.5%) were bought from Samchun Pure Chemical Co., Ltd. (Pyeongtaek, Korea). Ethyl alcohol ( $\text{C}_2\text{H}_5\text{OH}$ ,  $\geq 99.5\%$ ) was sourced from Duksan Pure Chemicals Co., Ltd. (Ansan-si, Korea). Deionized water (DI, 18.2 M $\Omega$  of resistivity) was obtained from a Direct-Q 3 UV system (Millipore, Billerica, MA, USA) and used in the preparation of all solutions. All the chemicals were used as received without further purification.

### 2.2. Preparation of PANI/ $\text{TiO}_2$ Photocatalyst

To prepare PANI (Figure 1) powder, 10 mL of 1 M HCl was added to 90 mL DI (Sol A). Sol B was prepared by dissolving 5 g of ammonium sulfate in 20 mL of Sol A. Sol C was prepared by adding 2 mL aniline to 80 mL of Sol A. Then, the mixture of Sol B and Sol C was stirred for 6 h. Afterward, the obtained precipitate was washed with 1000 mL DI and 100 mL ethanol. The washed PANI was dried in an oven (FTVO-701, Sci Finetech Co., Seoul, Korea) at 70 °C for 12 h. To prepare the PANI/ $\text{TiO}_2$  composite, 2 g  $\text{TiO}_2$  and 0.04, 0.08, 0.12, 0.16, and 0.20 g PANI (2%, 4%, 6%, 8%, and 10%, respectively) were added to 100 mL DI. After sonication of each mixture for 6 h, the PANI/ $\text{TiO}_2$  composites were oven-dried at 70 °C overnight before use.

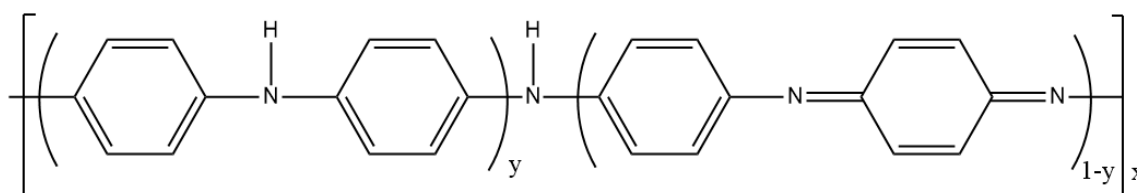


Figure 1. General formula of polyaniline.

### 2.3. Characterizations

To confirm the composition of PANI, the Fourier-transform infrared (FTIR) spectrum of PANI was recorded using a Nicolet iS50 FTIR apparatus equipped with an attenuated total reflectance accessory (Thermo Scientific, Waltham, MA, USA). Diffuse reflectance spectra (DRS) of pristine TiO<sub>2</sub> and the PANI/TiO<sub>2</sub> composite were measured using a diffuse reflectance UV–visible spectrophotometer (S-4100, Scinco Co., Ltd., Seoul, Korea) at a wavelength range of 200–800 nm and BaSO<sub>4</sub> powder as reference material. The morphology of the prepared PANI/TiO<sub>2</sub> sample was observed under a field-emission transmission electron microscope (FE-TEM; Tecnai G2 F30 S-Twin, FEI, Hillsboro, OR, USA). X-ray diffraction (XRD) pattern of 4% PANI/TiO<sub>2</sub> sample was obtained using high power X-ray diffractometer (D/max-2500V/PC, Rigaku, Tokyo, Japan).

### 2.4. Experimental Procedures

The photocatalysis experiments were conducted by degrading MB and BPA under visible-light irradiation. The photocatalyst concentration was adjusted to 0.8 g/L, under specified otherwise. The photocatalyst was sonicated in DI, and the suspension was spiked into 5 μM MB and 5 mg/L BPA solution, respectively. Aliquots of 1 mL were sampled and filtered through a 0.20-μm polytetrafluoroethylene (PTFE) filter (13JP020AN, Advantec, Tokyo, Japan) at a specific time. Six visible light lamps (4 W) were placed in a black acrylic box. A quartz reactor with a 420-nm cutoff filter was placed at 6 cm from the visible-light lamps. The light intensity was determined by Reinecke's salt actinometry (1.03 mW/cm<sup>2</sup>). The adsorption and the photolysis experiment were conducted without visible light and photocatalyst, respectively. To observe the reusability of the photocatalyst, a reuse test was conducted for four cycles. After each cycle, the sampled amount of solution was replenished for the next test. The photocatalytic activity was further assessed through a bacteriophage inactivation test by adding 5 mL of 4% PANI/TiO<sub>2</sub> suspension (4 g/L) to 10 mL of bacteriophage MS2 suspension (10<sup>5</sup> PFU/mL).

### 2.5. Analytical Methods

The residual MB concentration was analyzed using a UV–visible spectrophotometer (NEO-S2117, Neogen, Seoul, Korea) at a wavelength of 664 nm. BPA concentrations were analyzed using a YL 9100 high-performance liquid chromatography (HPLC) system (Young In Chromass, Anyang-si, Korea) equipped with a YL 9120 UV–visible detector, YL 9150 autosampler, and YL C18-4D column (4.6 mm × 150 mm, 5 μm). The ratio of the DI and acetonitrile in the mobile phase was 50:50 (*v/v*), which was eluted at a flow rate of 1 mL/min. The column temperature was 35 °C, and the BPA was detected at 230 nm. A plaque assay was used to measure the bacteriophage MS2 concentration, and the solution was 10,000-fold diluted in DI.

## 3. Results and Discussion

### 3.1. Characterization of PANI/TiO<sub>2</sub> Composite

The FTIR spectrum of prepared PANI and PANI/TiO<sub>2</sub> composite are shown in Figure 2. The peaks of PANI appeared at 788, 1292, 1481, and 1563/cm, which correspond to a 1,4 substitution pattern of the benzene ring, C–N stretching vibration of primary amines, C=C stretching vibrations of quinone and the benzene ring, and C=N stretching vibrations of quinone and the benzene ring, respectively [14,15]. This observation indicates that PANI was synthesized successfully. The broad band of the PANI/TiO<sub>2</sub> composite at 500/cm is attributed to the TiO<sub>2</sub> vibration [12]. Morphological observations of PANI/TiO<sub>2</sub> composite by TEM (Figure 3) revealed relatively small-sized TiO<sub>2</sub> particles dispersed and anchored on the PANI chain. The result of the TEM analysis suggests that PANI/TiO<sub>2</sub> composite was completely fabricated. XRD analyses were used to identify the crystalline structure of the PANI/TiO<sub>2</sub> composite (Figure 4). The characteristic peaks at 25.28, 37.80, 53.89 and 62.69 matched well with the (101), (004), (105) and (204) crystal planes of the synthetic anatase (JCPDS #21-1272) [16]. The crystal size estimated

by the Scherrer equation was about  $16.27 \pm 3.13$  nm [17,18], which was well matched with the size derived from the TEM image ( $16.59 \pm 3.59$  nm).

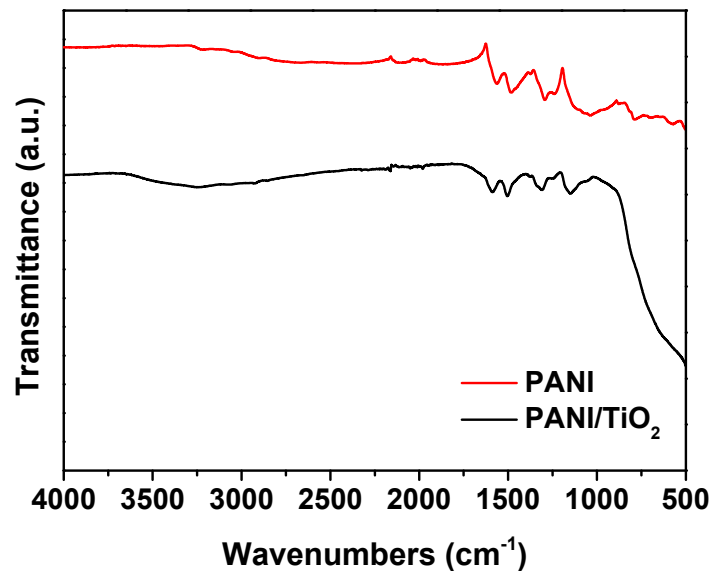


**Figure 2.** Fourier-transform infrared (FTIR) spectrum of prepared polyaniline (PANI) and PANI/TiO<sub>2</sub> composite.

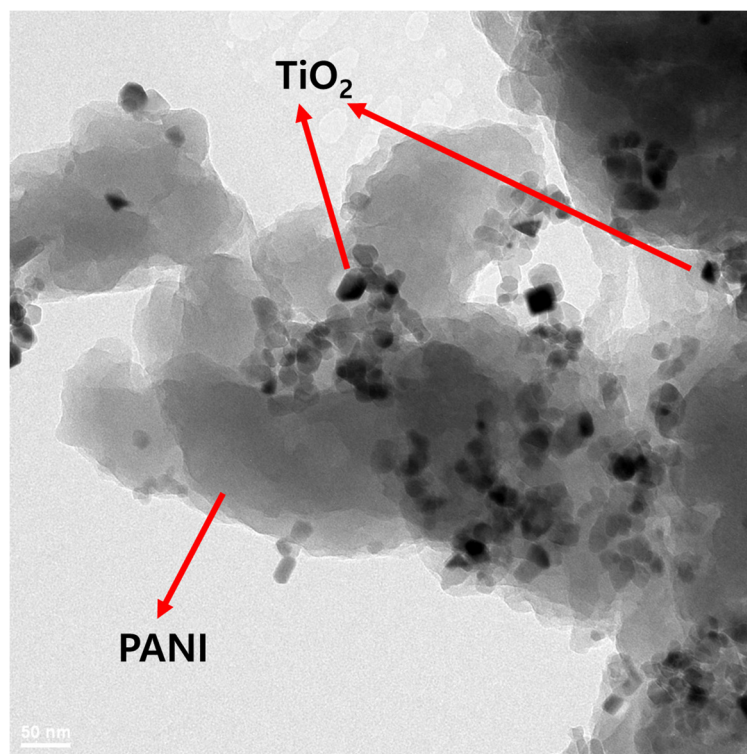


**Figure 3.** Field-emission transmission electron microscope (FE-TEM) image of PANI/TiO<sub>2</sub> composite.

The capacity to absorb light is an important factor for the activation of the visible-light photocatalyst [19]. To compare the light absorbance of the pristine TiO<sub>2</sub> and 4% PANI/TiO<sub>2</sub> composite in the visible-light region, DRS analysis was conducted in the wavelength range of 200–800 nm. The reflectance results (Figure 5) indicated a weaker photo-reflectance of 4% PANI/TiO<sub>2</sub> composite than TiO<sub>2</sub> at wavelengths above 400 nm, which means the composite has a stronger absorption

capacity of visible light and the possibility of photocatalytic activity under visible-light irradiation. The red-shift in the absorption edge of 4% PANI/TiO<sub>2</sub> in this study could be elucidated by a color change [20–22]. PANI/TiO<sub>2</sub> composites appeared blue and grayish, which had a positive effect on the visible-light absorption. By contrast, pristine TiO<sub>2</sub> powder was white. The band gap energies ( $E_g$ ) of samples were estimated from the intersection point of the absorption onsets and the baseline of the absorption spectrum using Kubelka–Munk remission function [2,23]. The  $E_g$  of pristine TiO<sub>2</sub> and PANI/TiO<sub>2</sub> composites were 3.21 and 3.15 eV, respectively. A similar band gap energy reduction in the PANI/TiO<sub>2</sub> composite (3.07 eV) has also been reported in the literature [12], which could lead to higher photocatalytic activity.

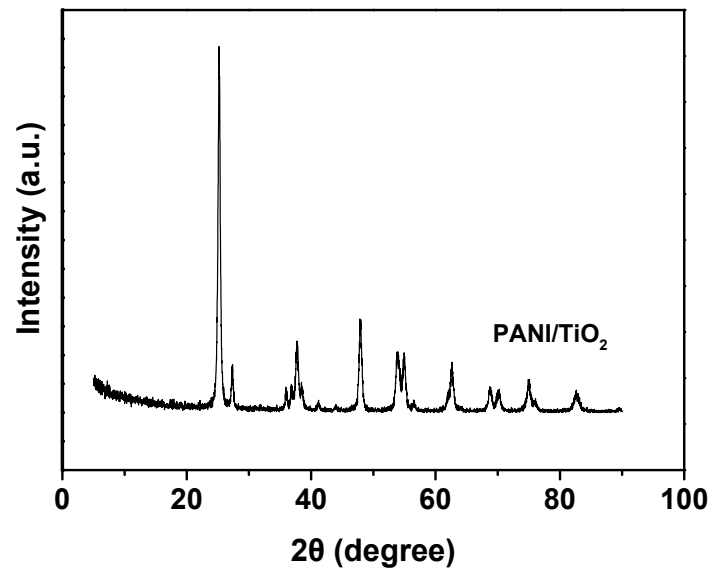


Figure 4. X-ray diffraction (XRD) pattern of PANI/TiO<sub>2</sub> composite.

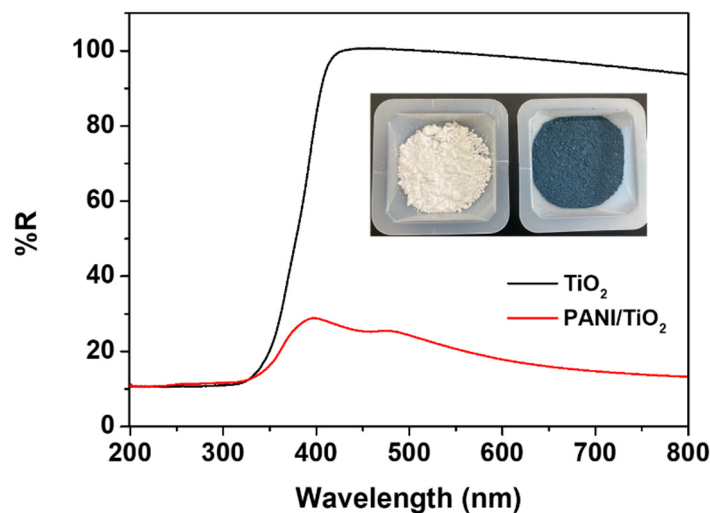
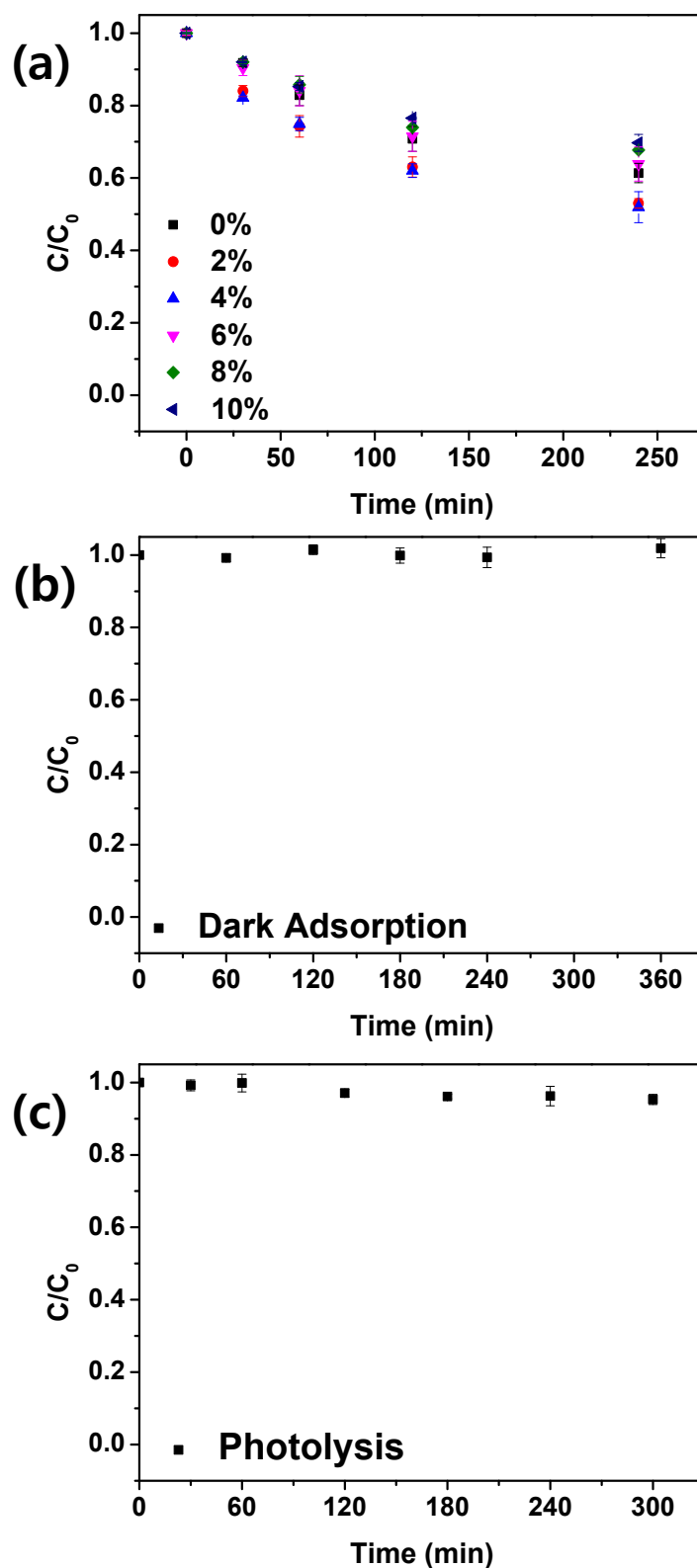


Figure 5. Diffuse reflectance spectra (DRS) spectra of TiO<sub>2</sub> and 4% PANI/TiO<sub>2</sub> composite (insert shows digital image of TiO<sub>2</sub> (left) and 4% PANI/TiO<sub>2</sub> composite (right)).

### 3.2. Photocatalytic Activity

To compare the effect of PANI composition in the PANI/TiO<sub>2</sub> composites, different weight ratios of PANI (2%, 4%, 6%, 8%, 10%) were added when the catalyst was prepared. Plots of  $C/C_0$  versus visible-light-irradiation time were constructed for the different catalysts (Figure 6a).



**Figure 6.** (a) Photocatalysis of methylene blue (MB) under visible-light irradiation with different photocatalysts, (b) dark adsorption of MB with 4% PANI/TiO<sub>2</sub>, and (c) photolysis of MB (MB = 5  $\mu$ M, catalyst dose: 0.8 g/L).

As the weight ratio of PANI increased from 0% to 4%, the degradation efficiency of MB increased from  $38.65 \pm 2.68\%$  to  $48.10 \pm 4.27\%$ , but with 10% PANI composition, it decreased to  $30.33 \pm 2.33\%$

in 240 min. This phenomenon shows that the proper amount of PANI is needed to optimize the degradation efficiency of a contaminant owing to obstruction of the molecular structure of PANI [24]. As a result, 4% PANI/TiO<sub>2</sub> composite displayed enhanced photocatalytic activity compared with commercial TiO<sub>2</sub> under visible-light irradiation. This is due to the synergetic effect of the well-matched energy levels of TiO<sub>2</sub> and PANI, PANI/TiO<sub>2</sub> composite could interfere the recombination of holes and electrons, which can improve the production of the reactive oxygen species that degrades MB. In addition, since PANI is a photosensitizer with a narrow bandgap, PANI/TiO<sub>2</sub> composite could enhance the response to visible light by inserting the energy level of PANI into the energy level of TiO<sub>2</sub>, which was consistent with the DRS result. These electron transfer between the PANI and TiO<sub>2</sub> semiconductors and the enhanced photocatalytic activity of the composites has already been reported experimentally in other literature [12,25]. Adsorption of MB by the 4% PANI/TiO<sub>2</sub> did not occur (Figure 6b), and the direct photolysis of MB by visible-light irradiation was relatively low ( $4.69 \pm 1.67\%$ , Figure 6c), indicating that MB degraded predominantly by photocatalytic activity.

Different amounts of 4% PANI/TiO<sub>2</sub> (0, 0.32, 0.8, 1.12, 1.6 g/L) were added to the MB solution to optimize the catalyst dose. Results of the removal ratio of MB by different photocatalyst doses (Figure 7) showed that MB degradation increased from  $3.88 \pm 1.51\%$  to  $67.37 \pm 7.82\%$  as the dose of the photocatalyst increased to 1.12 g/L but adversely decreased to  $58.40 \pm 0.38\%$  at the dose of 1.6 g/L. This result could be explained in terms of photocatalyst agglomeration and visible-light penetration into the suspension [26]. As the photocatalyst concentration in the solution is increased, the photocatalyst tends to agglomerate, which will reduce the amount of photocatalyst surface exposed to the visible-light. Furthermore, the agglomeration and sedimentation of photocatalyst particles also decrease the penetration depth of visible light from the reactor wall, causing light scattering, which lowers the light intensity entering the suspension.

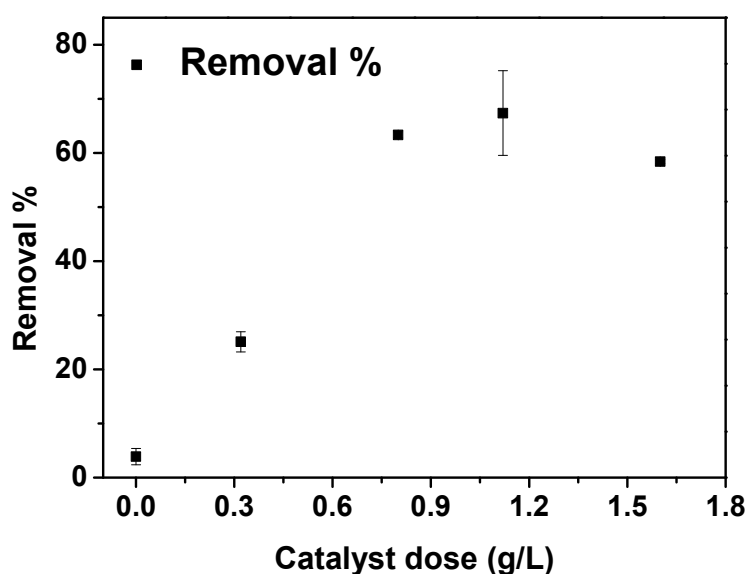


**Figure 7.** Removal ratios of MB by 4% PANI/TiO<sub>2</sub> with different catalyst doses under visible-light irradiation (MB = 5 μM).

### 3.3. Application to BPA and Bacteriophage MS2 Degradation

When the optimized PANI/TiO<sub>2</sub> composite was applied to the photocatalytic degradation of 5 mg/L BPA, BPA was degraded by  $80 \pm 0.75\%$  in 360 min (Figure 8a). To calculate the degradation rate ( $k_{app}$ ), the pseudo-first-order degradation kinetics of BPA by PANI/TiO<sub>2</sub> were plotted (Figure 8b) to solve Equation (1): [27]

$$\ln(C_0/C) = k_{app}t \quad (1)$$

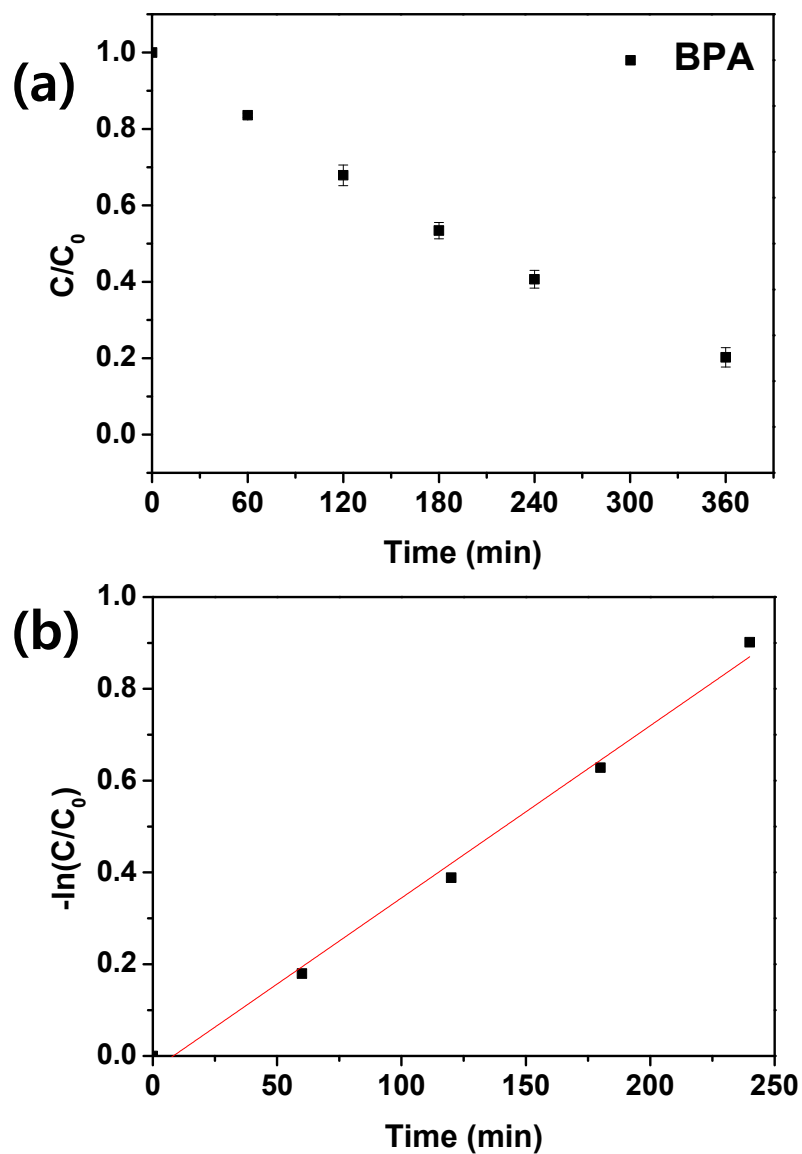


**Figure 8.** (a) Degradation of bisphenol A (BPA) by 4% PANI/TiO<sub>2</sub> under visible-light irradiation, and (b) pseudo-first-order kinetics of BPA degradation (BPA = 5 mg/L, catalyst dose: 0.8 g/L).

BPA had a rate constant of  $0.00375 \pm 0.00018/\text{min}$ , and the correlation coefficient ( $R^2$ ) was 0.99, which indicates that BPA degradation by PANI/TiO<sub>2</sub> follows pseudo-first-order kinetics.

Bacteriophages are potential indicator organisms for the efficiency of treatment processes because they are characterized by their stability to sunlight, temperature, and chemical/physical treatments [28]. PANI/TiO<sub>2</sub> degraded 96.2% of bacteriophage MS2 in 120 min under visible-light irradiation (Figure 9). The first-order rate constant of bacteriophage MS2 was  $0.02637 \pm 0.0055/\text{min}$ . These results highlight the applicability of PANI/TiO<sub>2</sub> for the removal of recalcitrant organic compounds and bacteriophages.

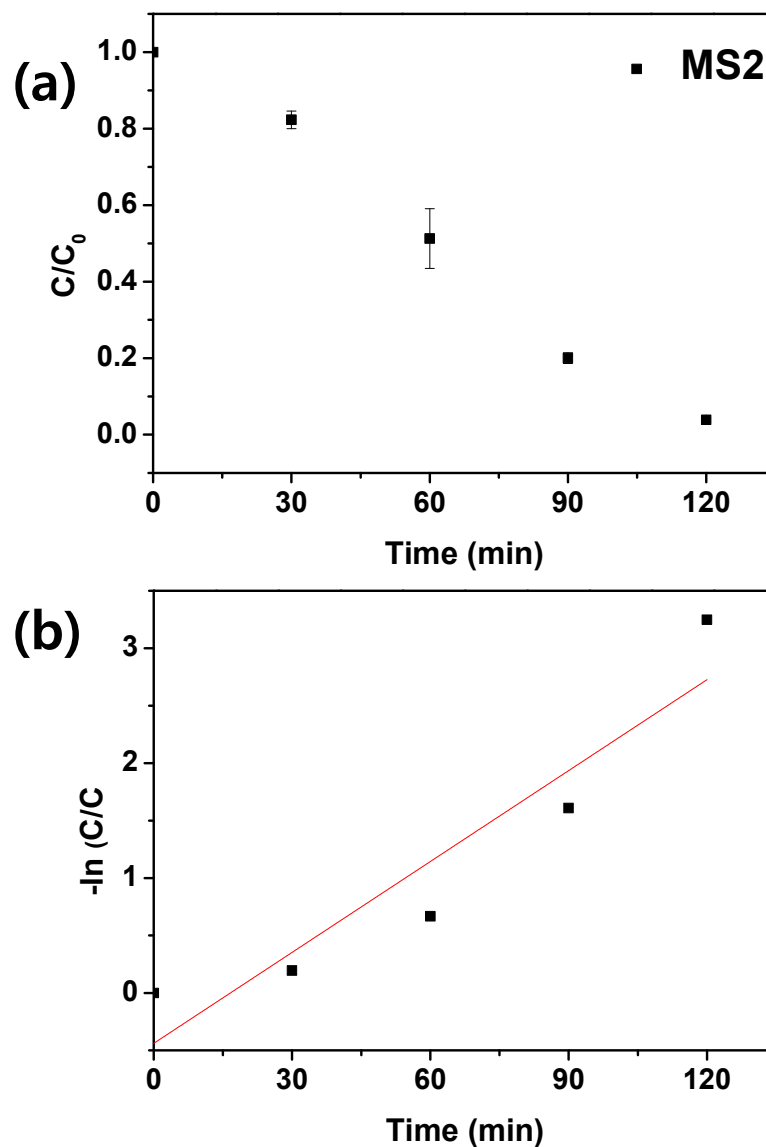


**Figure 9.** (a) Degradation of bacteriophage MS2 by 4% PANI/TiO<sub>2</sub> under visible-light irradiation, and (b) pseudo-first-order kinetics of MS2 degradation (MS2 = 10<sup>5</sup> CFU/mL, catalyst dose: 1.33 g/L).

### 3.4. Reusability

For practical applications, the reusability of photocatalysts is important as it is related to the stability of the photocatalyst [29]. The reuse test was conducted for four cycles under visible-light irradiation to investigate the stability of PANI/TiO<sub>2</sub>. After the photocatalytic reaction, the catalyst was reused for the next cycle, and the degradation efficiency was determined by analyzing the concentrations of MB residue in the samples. After four reuses, more than 99% of MB was degraded by PANI/TiO<sub>2</sub> in 360 min under visible-light irradiation (Figure 10). PANI/TiO<sub>2</sub> did not show any notable loss of photocatalytic activity, suggesting that it remains stable during the degradation of MB. It also suggests that active sites of PANI/TiO<sub>2</sub> were not occupied by the adsorption of MB molecules because MB might be oxidized by the continuously generated reactive oxygen species on the surface of PANI/TiO<sub>2</sub> [30].

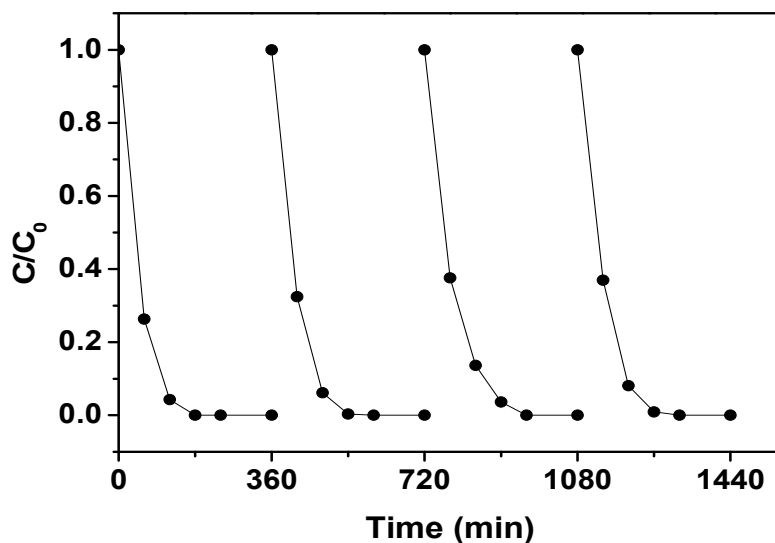


**Figure 10.** Reuse of 4% PANI/TiO<sub>2</sub> for degradation of MB under visible-light irradiation (MB = 5 μM, catalyst dose: 0.8 g/L).

#### 4. Conclusions

In this study, a PANI/TiO<sub>2</sub> composite with enhanced visible-light photocatalytic activity was prepared. The results indicated that the PANI ratio and the amount of PANI/TiO<sub>2</sub> dose were important factors in the photocatalytic performance of PANI/TiO<sub>2</sub>. A 4% PANI ratio and 1.12 g/L PANI/TiO<sub>2</sub> dose were most suitable for MB degradation. The degradation of BPA and bacteriophage MS2 by PANI/TiO<sub>2</sub> reached 96.2% in 120 min and 80% in 360 min. The photocatalytic activity of PANI/TiO<sub>2</sub> did not show any noticeable decrease, indicating the high stability of PANI/TiO<sub>2</sub>. In conclusion, PANI/TiO<sub>2</sub> is an enhanced visible-light-activated photocatalyst for the degradation and removal of contaminants.

**Author Contributions:** Conceptualization, S.-J.P. and C.-G.L.; Methodology, H.S.L. and Y.-J.L.; Validation, Y.-J.L.; Formal Analysis, H.S.L. and Y.-J.L.; Data Curation, J.L.; Visualization, Y.-J.L.; Supervision, S.J. and G.-A.S.; Writing—Original Draft Preparation, Y.-J.L. and C.-G.L.; Writing—Review & Editing, S.-J.P. and C.-G.L. All authors have read and agreed to the published version of the manuscript.

**Funding:** This research was supported by the Ajou University Research Fund.

**Conflicts of Interest:** The authors declare no conflict of interest.

#### References

1. Fujishima, A.; Honda, K. Electrochemical Photolysis of Water at a Semiconductor Electrode. *Nature* **1972**, *238*, 37–38. [[CrossRef](#)] [[PubMed](#)]
2. Lee, Y.-J.; Kang, J.-K.; Park, S.-J.; Lee, C.-G.; Moon, J.-K.; Alvarez, P.J.J. Photocatalytic degradation of neonicotinoid insecticides using sulfate-doped Ag<sub>3</sub>PO<sub>4</sub> with enhanced visible light activity. *Chem. Eng. J.* **2020**, *402*, 126183. [[CrossRef](#)]
3. Lee, C.-G.; Javed, H.; Zhang, D.; Kim, J.; Westerhoff, P.; Li, Q.; Alvarez, P.J.J. Porous Electrospun Fibers Embedding TiO<sub>2</sub> for Adsorption and Photocatalytic Degradation of Water Pollutants. *Environ. Sci. Technol.* **2018**, *52*, 4285–4293. [[CrossRef](#)] [[PubMed](#)]
4. Habib, Z.; Lee, C.-G.; Li, Q.; Khan, S.J.; Ahmad, N.M.; Jamal, Y.; Huang, X.; Javed, H. Bi-Polymer Electrospun Nanofibers Embedding Ag<sub>3</sub>PO<sub>4</sub>/P25 Composite for Efficient Photocatalytic Degradation and Anti-Microbial Activity. *Catalyst* **2020**, *10*, 784. [[CrossRef](#)]
5. Olad, A.; Behboudi, S.; Entezami, A.A. Preparation, characterization and photocatalytic activity of TiO<sub>2</sub>/polyaniline core-shell nanocomposite. *Bull. Mater. Sci.* **2012**, *35*, 801–809. [[CrossRef](#)]
6. Ghosh, S.; Kouamé, N.A.; Ramos, L.; Rémita, S.; Dazzi, A.; Deniset-Besseau, A.; Beaunier, P.; Goubard, F.; Aubert, P.-H.; Remita, H. Conducting polymer nanostructures for photocatalysis under visible light. *Nat. Mater.* **2015**, *14*, 505–511. [[CrossRef](#)]

7. Park, H.; Park, Y.; Kim, W.; Choi, W. Surface modification of TiO<sub>2</sub> photocatalyst for environmental applications. *J. Photochem. Photobiol. C Photochem. Rev.* **2013**, *15*, 1–20. [[CrossRef](#)]
8. Wang, C.; Wang, L.; Jin, J.; Liu, J.; Li, Y.; Wu, M.; Chen, L.; Wang, B.; Yang, X.-Y.; Su, B.-L. Probing effective photocorrosion inhibition and highly improved photocatalytic hydrogen production on monodisperse PANI@CdS core-shell nanospheres. *Appl. Catal. B Environ.* **2016**, *188*, 351–359. [[CrossRef](#)]
9. Yang, Y.; Wen, J.; Wei, J.; Xiong, R.; Shi, J.; Pan, C. Polypyrrole-Decorated Ag-TiO<sub>2</sub> Nanofibers Exhibiting Enhanced Photocatalytic Activity under Visible-Light Illumination. *ACS Appl. Mater. Interfaces* **2013**, *5*, 6201–6207. [[CrossRef](#)]
10. Zhu, Y.; Xu, S.; Yi, D. Photocatalytic degradation of methyl orange using polythiophene/titanium dioxide composites. *React. Funct. Polym.* **2010**, *70*, 282–287. [[CrossRef](#)]
11. Chhabra, V.A.; Kaur, R.; Walia, M.S.; Kim, K.-H.; Deep, A. PANI/PbS QD nanocomposite structure for visible light driven photocatalytic degradation of rhodamine 6G. *Environ. Res.* **2020**, *186*, 109615. [[CrossRef](#)]
12. Li, X.; Wang, D.; Cheng, G.; Luo, Q.; An, J.; Wang, Y. Preparation of polyaniline-modified TiO<sub>2</sub> nanoparticles and their photocatalytic activity under visible light illumination. *Appl. Catal. B Environ.* **2008**, *81*, 267–273. [[CrossRef](#)]
13. Lee, S.L.; Chang, C.-J. Recent Developments about Conductive Polymer Based Composite Photocatalysts. *Polymers* **2019**, *11*, 206. [[CrossRef](#)] [[PubMed](#)]
14. Abdolahi, A.; Hamzah, E.; Ibrahim, Z.; Hashim, S. Synthesis of Uniform Polyaniline Nanofibers through Interfacial Polymerization. *Materials* **2012**, *5*, 1487–1494. [[CrossRef](#)]
15. Deshmukh, M.A.; Gicevicius, M.; Ramanaviciene, A.; Shirsat, M.D.; Viter, R.; Ramanavicius, A. Hybrid electrochemical/electrochromic Cu(II) ion sensor prototype based on PANI/ITO-electrode. *Sens. Actuators B Chem.* **2017**, *248*, 527–535. [[CrossRef](#)]
16. Cheng, X.; Shang, Y.; Cui, Y.; Shi, R.; Zhu, Y.; Yang, P. Enhanced photoelectrochemical and photocatalytic properties of anatase-TiO<sub>2</sub>(B) nanobelts decorated with CdS nanoparticles. *Solid State Sci.* **2020**, *99*, 106075. [[CrossRef](#)]
17. Borchert, H.; Shevchenko, E.V.; Robert, A.; Mekis, I.; Kornowski, A.; Grübel, A.G.; Weller, H. Determination of Nanocrystal Sizes: A Comparison of TEM, SAXS, and XRD Studies of Highly Monodisperse CoPt<sub>3</sub>Particles. *Langmuir* **2005**, *21*, 1931–1936. [[CrossRef](#)] [[PubMed](#)]
18. Lee, C.-G.; Lee, S.; Park, J.-A.; Park, C.; Lee, S.-J.; Kim, S.-B.; An, B.; Yun, S.-T.; Lee, S.-H.; Choi, J.-W. Removal of copper, nickel and chromium mixtures from metal plating wastewater by adsorption with modified carbon foam. *Chemosphere* **2017**, *166*, 203–211. [[CrossRef](#)] [[PubMed](#)]
19. Wu, X.; Cao, L.; Song, J.; Si, Y.; Yu, J.; Ding, B. Thorn-like flexible Ag<sub>2</sub>C<sub>2</sub>O<sub>4</sub>/TiO<sub>2</sub> nanofibers as hierarchical heterojunction photocatalysts for efficient visible-light-driven bacteria-killing. *J. Colloid Interface Sci.* **2020**, *560*, 681–689. [[CrossRef](#)]
20. Fan, L.; Liu, Z.; Zhu, Y.; Wang, Z.; Zhao, S.; Zhu, L.; Zhang, Q. Synthesis of Li-doping tetragonal-Bi<sub>2</sub>O<sub>3</sub> nanomaterial with high efficient visible light photocatalysis. *J. Mater. Sci. Mater. Electron.* **2020**, *31*, 2100–2110. [[CrossRef](#)]
21. Jo, W.-K.; Moru, S.; Tonda, S. Magnetically responsive SnFe<sub>2</sub>O<sub>4</sub>/g-C<sub>3</sub>N<sub>4</sub> hybrid photocatalysts with remarkable visible-light-induced performance for degradation of environmentally hazardous substances and sustainable hydrogen production. *Appl. Surf. Sci.* **2020**, *506*, 144939. [[CrossRef](#)]
22. Hu, J.; Li, J.; Cui, J.; An, W.; Liu, L.; Liang, Y.; Cui, W. Surface oxygen vacancies enriched FeOOH/Bi<sub>2</sub>MoO<sub>6</sub> photocatalysis-fenton synergy degradation of organic pollutants. *J. Hazard. Mater.* **2020**, *384*, 121399. [[CrossRef](#)] [[PubMed](#)]
23. Tallapally, V.; Nakagawara, T.A.; Demchenko, D.O.; Ozgur, U.; Arachchige, I.U. Ge<sub>1-x</sub>Sn<sub>x</sub> alloy quantum dots with composition-tunable energy gaps and near-infrared photoluminescence. *Nanoscale* **2018**, *10*, 20296–20305. [[CrossRef](#)]
24. Zhang, Y.; Selvaraj, R.; Kim, Y.; Sillanpää, M.; Tai, C.-W. Photo-corrosion inhibition of Ag<sub>3</sub>PO<sub>4</sub> by polyaniline coating. *Desalin. Water Treat.* **2015**, *57*, 1–10. [[CrossRef](#)]
25. Yang, C.; Dong, W.; Cui, G.; Zhao, Y.; Shi, X.; Xia, X.; Tang, B.; Wang, W. Enhanced photocatalytic activity of PANI/TiO<sub>2</sub> due to their photosensitization-synergetic effect. *Electrochim. Acta* **2017**, *247*, 486–495. [[CrossRef](#)]
26. Jantawasu, P.; Sreethawong, T.; Chavadej, S. Photocatalytic activity of nanocrystalline mesoporous-assembled TiO<sub>2</sub> photocatalyst for degradation of methyl orange monoazo dye in aqueous wastewater. *Chem. Eng. J.* **2009**, *155*, 223–233. [[CrossRef](#)]

27. Wang, Z.; Wang, Y.; Huang, L.; Liu, X.; Han, Y.; Wang, L. La<sub>2</sub>Zr<sub>2</sub>O<sub>7</sub>/rGO synthesized by one-step sol-gel method for photocatalytic degradation of tetracycline under visible-light. *Chem. Eng. J.* **2020**, *384*, 123380. [[CrossRef](#)]
28. Venieri, D.; Gounaki, I.; Binas, V.; Zachopoulos, A.; Kiriakidis, G.; Mantzavinos, D. Inactivation of MS2 coliphage in sewage by solar photocatalysis using metal-doped TiO<sub>2</sub>. *Appl. Catal. B Environ.* **2015**, *178*, 54–64. [[CrossRef](#)]
29. Singh, P.; Mondal, K.; Sharma, A. Reusable electrospun mesoporous ZnO nanofiber mats for photocatalytic degradation of polycyclic aromatic hydrocarbon dyes in wastewater. *J. Colloid Interface Sci.* **2013**, *394*, 208–215. [[CrossRef](#)]
30. Fouad, K.; Alalm, M.G.; Bassyouni, M.; Saleh, M.Y. A novel photocatalytic reactor for the extended reuse of W-TiO<sub>2</sub> in the degradation of sulfamethazine. *Chemosphere* **2020**, *257*, 127270. [[CrossRef](#)]



© 2020 by the authors. Licensee MDPI, Basel, Switzerland. This article is an open access article distributed under the terms and conditions of the Creative Commons Attribution (CC BY) license (<http://creativecommons.org/licenses/by/4.0/>).